Asian Journal of Organic Chemistry

Supporting Information

Dual Photosensitizer Cycles Working Synergistically in a C(sp)-C(sp^3) Cross-Coupling Reaction

Megan Amy Bryden, Marco Villa, Andrea Fermi, Paola Ceroni,* and Eli Zysman-Colman*

Table of Contents

Experimental Section

General Synthetic Procedures. The following starting materials were synthesised according to literature procedures: **pDTCz-DPmS**,[1] Hantzsch ester (HE),[2] (bromoethynyl)benzene[3] and 1.3-dioxoisoindolin-2-yl cyclohexanecarboxylate.[4] All other reagents and solvents were obtained from commercial sources and used as received. Air-sensitive reactions were performed under a nitrogen atmosphere using Schlenk techniques, no special precautions were taken to exclude air or moisture during work-up and crystallisation. Anhydrous THF was obtained from a MBraun SPS5 solvent purification system. Flash column chromatography was carried out using silica gel (Silia-P from Silicycle, 60 Å, 40-63 μm). Analytical thin-layer-chromatography (TLC) was performed with silica plates with aluminum backings (250 μm with F-254 indicator). TLC visualization was accomplished by 254/365 nm UV lamp. ^{1}H and spectra were recorded on a Bruker Advance spectrometer (500 or 400 MHz for ^{1}H). The following abbreviations have been used for multiplicity assignments: "s" for singlet, "d" for doublet, "t" for triplet, "q" for quartet and "m" for multiplet. ^{1}H NMR spectra were referenced residual solvent peaks with respect to TMS (δ = 0 ppm).

Photophysical measurements. Optically dilute solutions of concentrations on the order of 10^{-5} or 10^{-6} M of the photocatalysts were prepared in spectroscopic or HPLC grade solvents for absorption and emission analysis. Absorption spectra were recorded at room temperature on a Varian Cary 50 BIO spectrophotometer with a 1 cm quartz cuvette or a Hellma ultra-micro cuvette with 3 mm optical path length. Degassed solutions were prepared via four freeze-pump-thaw cycles and spectra were taken using home-made Schlenk quartz cuvette. Steady-state emission, excitation spectra and time-resolved emission spectra were recorded at 298 K using an Edinburgh Instruments F980 or a Perkin Elmer LS55 spectrofluorometer, equipped with a Hamamatsu R928 phototube. Samples were excited at 390 nm for steady-state measurements and at 340 nm for time-resolved measurements.

Fitting of time-resolved luminescence measurements: Time-resolved PL measurements were fitted to a sum of exponentials decay model, with chi-squared (χ^2) values between 1 and 2, using the EI FLS980 or Edinburgh FLS920 software. Each component of the decay is assigned a weight, (w_i), which is the contribution of the emission from each component to the total emission. The error in the calculation of the quenching constant is 20%. All the experiments relative to HE quenching were recorded at high concentration in a small volume cell 3mm × 3mm and the quenching constant are evaluated on the emission intensity.

Photoluminescence quantum yield measurements: Photoluminescence quantum yields were measured following the method of Demas and Crosby[5] using $[Ru(bpy)_3]^{2+}$ as the standard in air-equilibrated aqueous solution $\Phi = 0.0405$.[6]

Photocatalysis

Photocatalysis experiments were conducted using a custom-built photoreactor, as shown in Figure **S1**, allowing for up to 8 parallel photochemical reactions (7 mL) at a time. The photochemistry reaction chamber is filled with mirrors to evenly distribute light. The reactor is placed upon a magnetic stirrer plate allowing for reactions to be completed with stirring. Reactions are irradiated using Kessil PR160 and PR160L LED sources. For Kessil PR160-390 nm and PR160L-427 nm, the power consumption maximum is 52 W and 45 W, respectively, with the average intensity measured from 1 cm distance being 399 mW cm^{-2}. The intensity on each lamp is tuneable, with the maximum intensity selected for all photocatalytic reactions. A cooling fan is directed at the photoreactor to ensure the reaction mixture maintains at room temperature, which is further guaranteed by the presence of two fans on the photoreactor itself.

After the photoreactions were completed, the products were analysed by ^{1}H NMR spectroscopy using 1,3,5-trimethoxybenzene as an internal standard. All yields shown represent the mean yield from at least two reactions with the associated standard deviation.

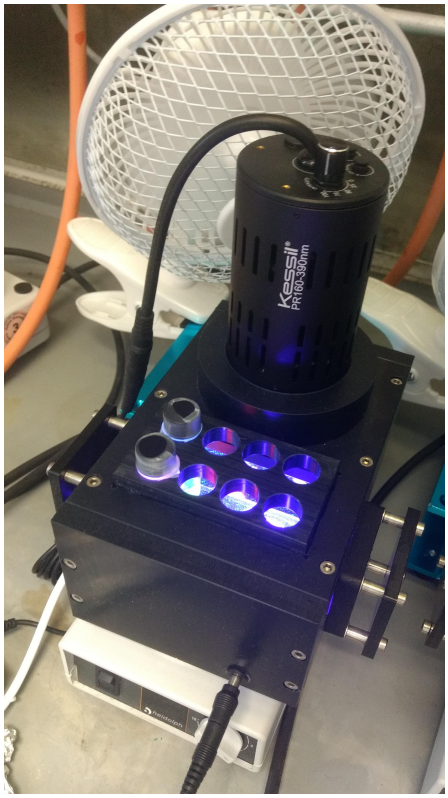

Figure **S1**. Experimental set-up for photocatalysis reactions.

Procedure for C(sp)-C(sp^3) cross coupling reaction.

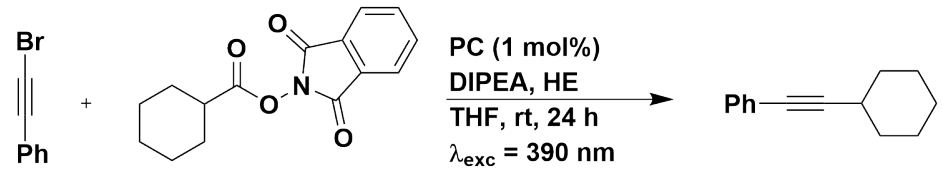

Figure **S2**. Reaction scheme for the C(sp)-C(sp^3) cross-coupling reaction.

To a 7 mL oven-dried vial was added (bromoethynyl)benzene (0.036 mL, 0.3 mmol, 1.5 equiv.), 1,3-dioxoisoindolin-2-yl cyclohexanecarboxylate (55 mg, 0.2 mmol, 1 equiv.), PC (0.002 mmol, 0.01 equiv., 1 mol%) and Hantzsch ester (76 mg, 0.3 mmol, 1.5 equiv.). The vial was purged with N_2 for 5 min and dry THF (1.0 mL) was added followed by DIPEA (0.070 mL, 0.4 mmol, 2.0 equiv.). The vial was purged with N_2 for a further 10 min. The vial was then irradiated with Kessil lamp (λ_{exc} = 390 nm or 427 nm) at room temperature with stirring for 24 h. The mixture was concentrated in vacuo and the crude mixture analysed by ^{1}H NMR spectroscopy using 1,3,5-trimethoxybenzene as the internal standard.

UV-Vis absorption spectra

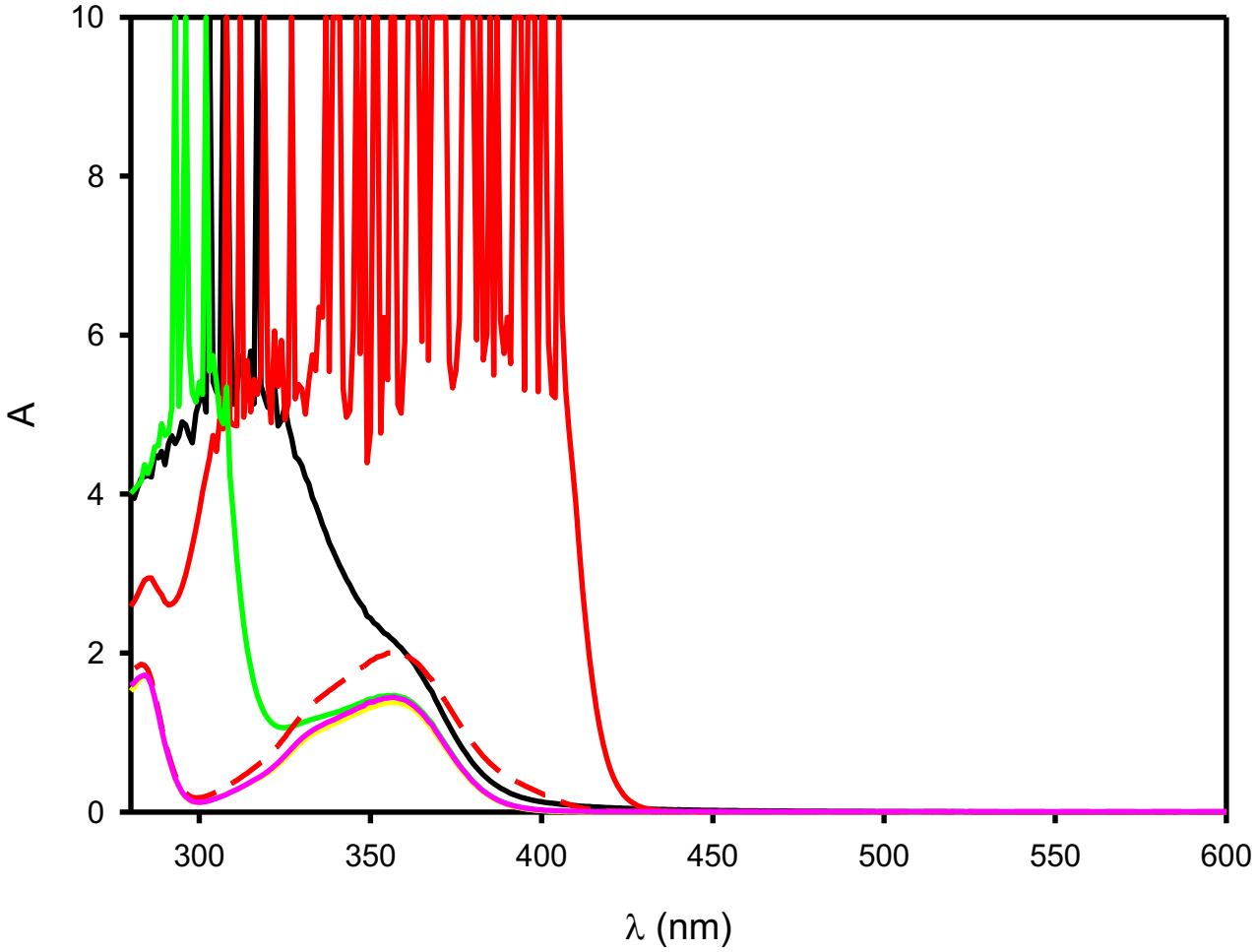

Figure **S3**. UV-Vis absorption spectra of a 4.27×10^{-5} M solution of **pDTCz-DPmS** in THF (yellow) and after the addition of PhCCBr (black, 3.7 mM), HE (red, 3.9 mM), NHPI (green, 4.1 mM), DIPEA (purple, 3.5 mM) and HE (red dashed, 52 μM).

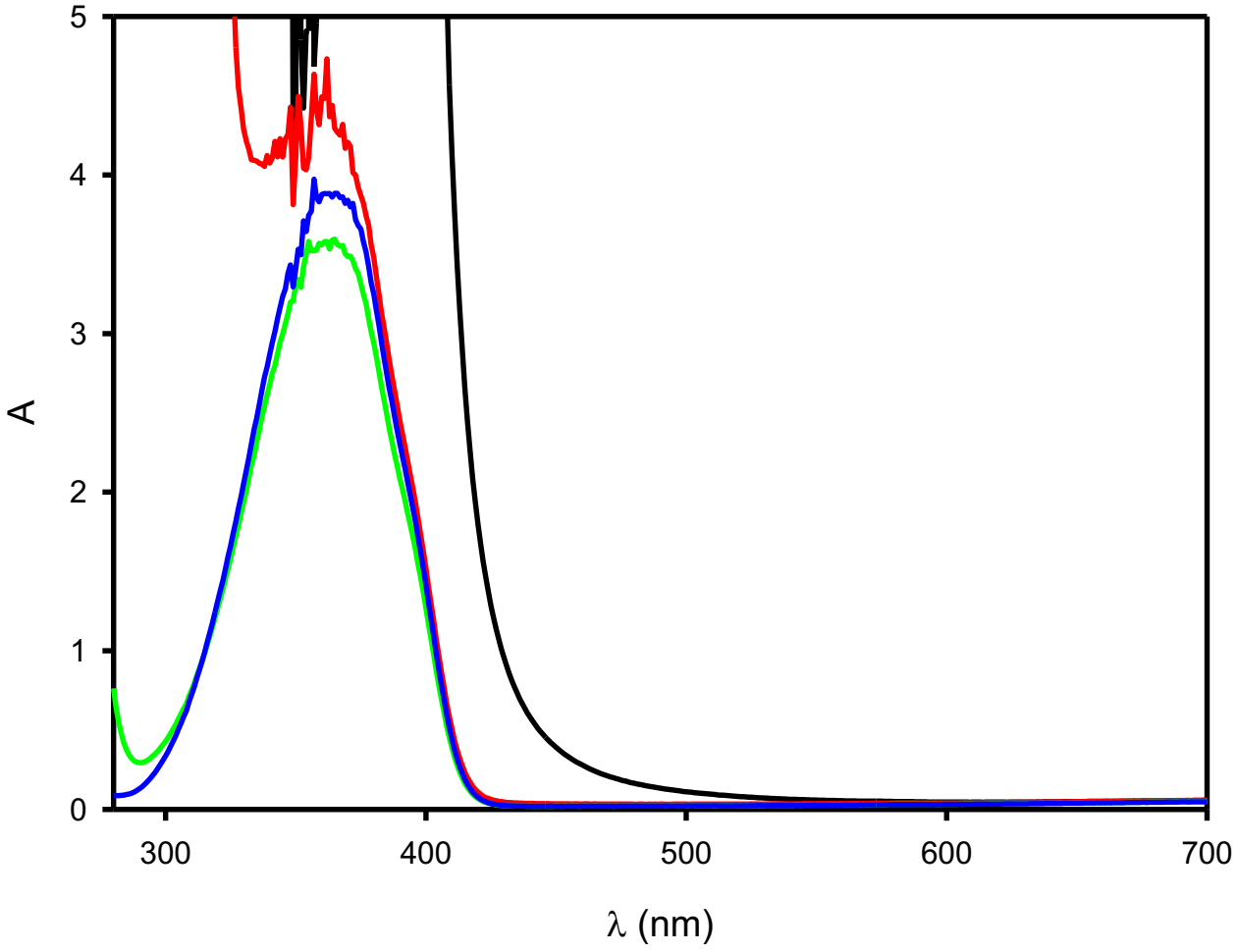

Figure **S4**. UV-Vis absorption spectra of a 2.55×10^{-3} M solution of HE in THF (blue) and after the addition of PhCCBr (black, 200 mM), NHPI (red, 300 mM), DIPEA (green, 400 mM).

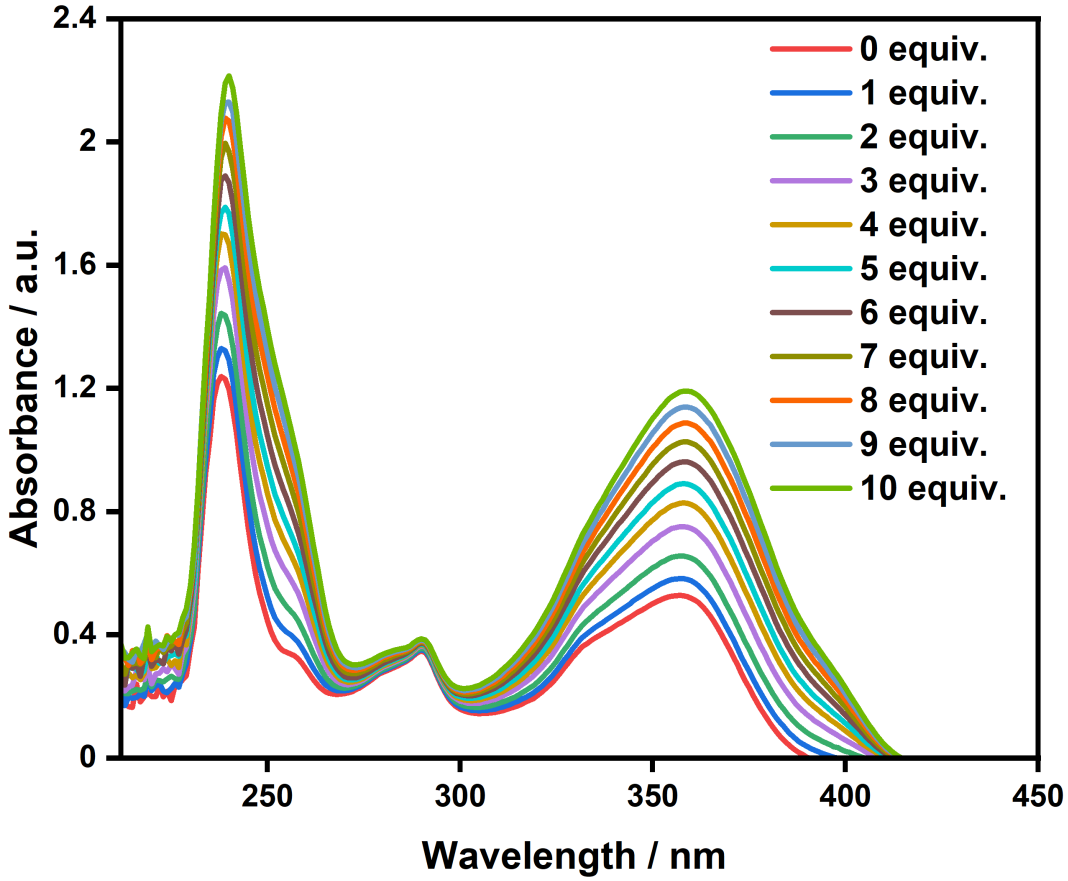

Figure **S5**. UV-Vis absorption spectra of **pDTCz-DPmS** in THF with increasing equivalents of HE from 0 to 10.

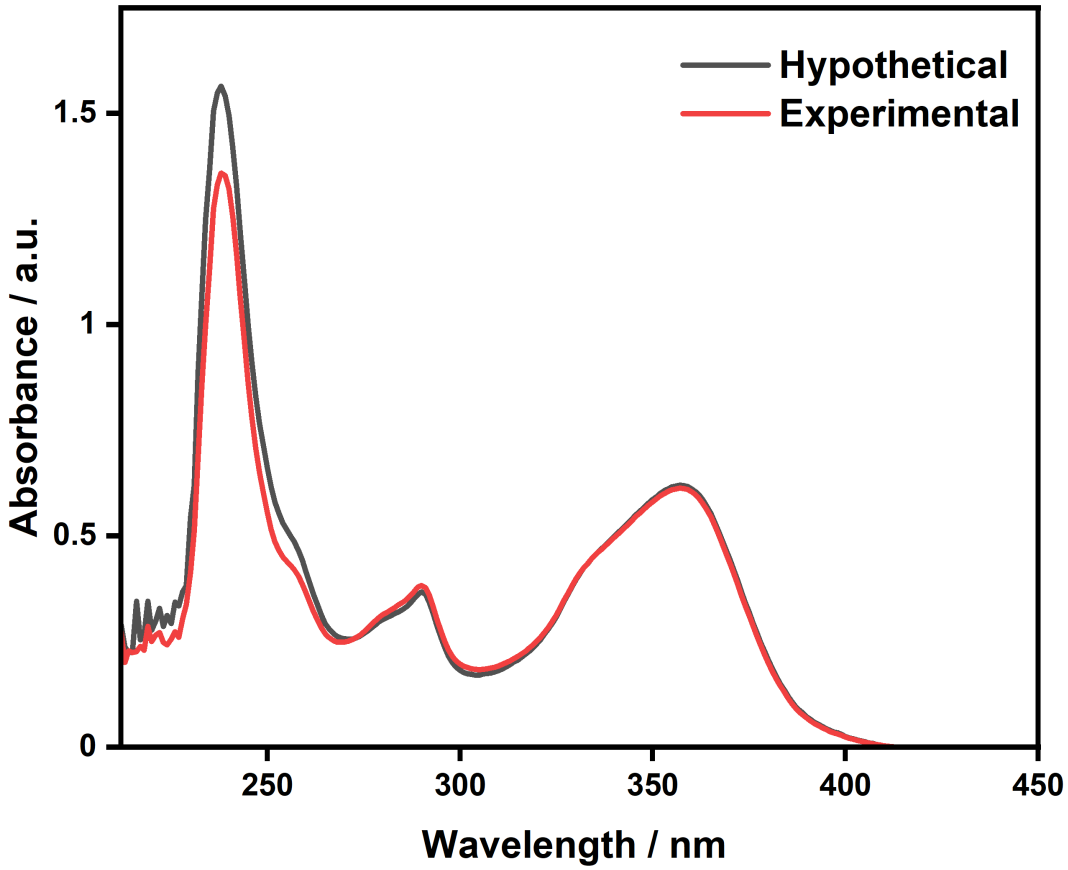

Figure **S6**. Hypothetical and experimental UV-Vis spectra of the 1:1 ratio of **pDTCz-DPmS** and HE in THF.

To ensure that there was no EDA complex forming between **pDTCz-DPmS** and HE, the UV-vis absorption spectrum of **pDTCz-DPmS** was monitored with the addition of increasing equivalents of HE. As shown in Figure **S5**, the CT band of **pDTCz-DPmS** (and the peak at ~240 nm) does indeed increase with increasing amounts of HE. However, the UV-Vis absorption spectra are additive, reflecting only the superposition of the absorption spectra **pDTCz-DPmS** and HE. To test this, we measured the UV-Vis absorption spectra of HE at the exact same concentration as **pDTCz-DPmS** and then added these two UV-Vis absorption spectra to obtain a hypothetical UV-Vis absorption for the two species. We then compared this to the experimental UV-Vis absorption spectrum we obtained when measuring a 1:1 solution of **pDTCz-DPmS** and HE. As shown in Figure **S6**, the hypothetical and experimental UV-Vis absorption

spectra overlap almost identically, implying that there is no interaction between **pDTCz-DPmS** and HE in the ground state.

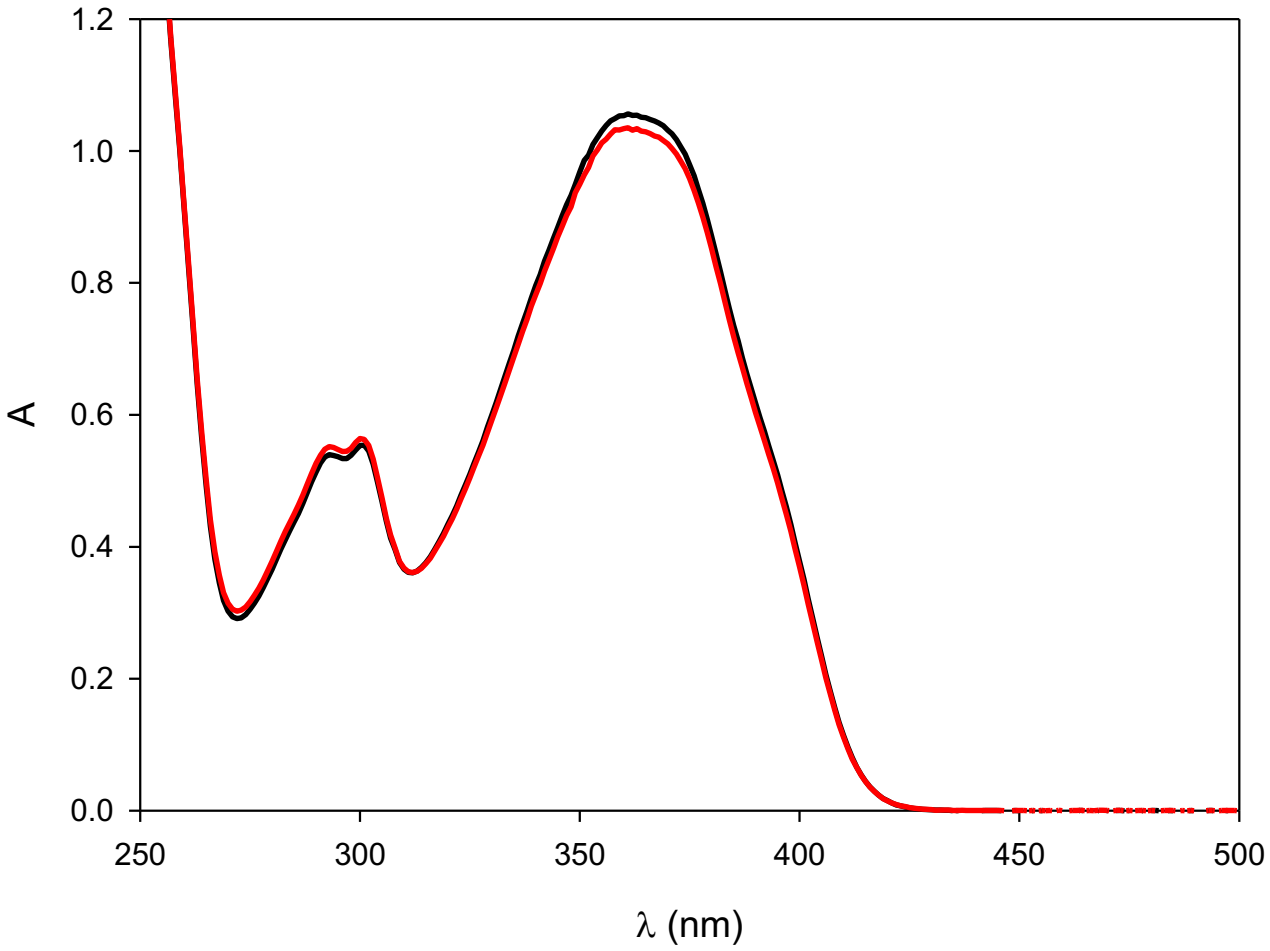

Figure **S7**. UV-Vis absorption spectra of a 10^{-4} M solution of NHPI and HE recorded with a two-chamber cuvette, before (black line) and after mixing the two solutions (red line).

Steady-state PL

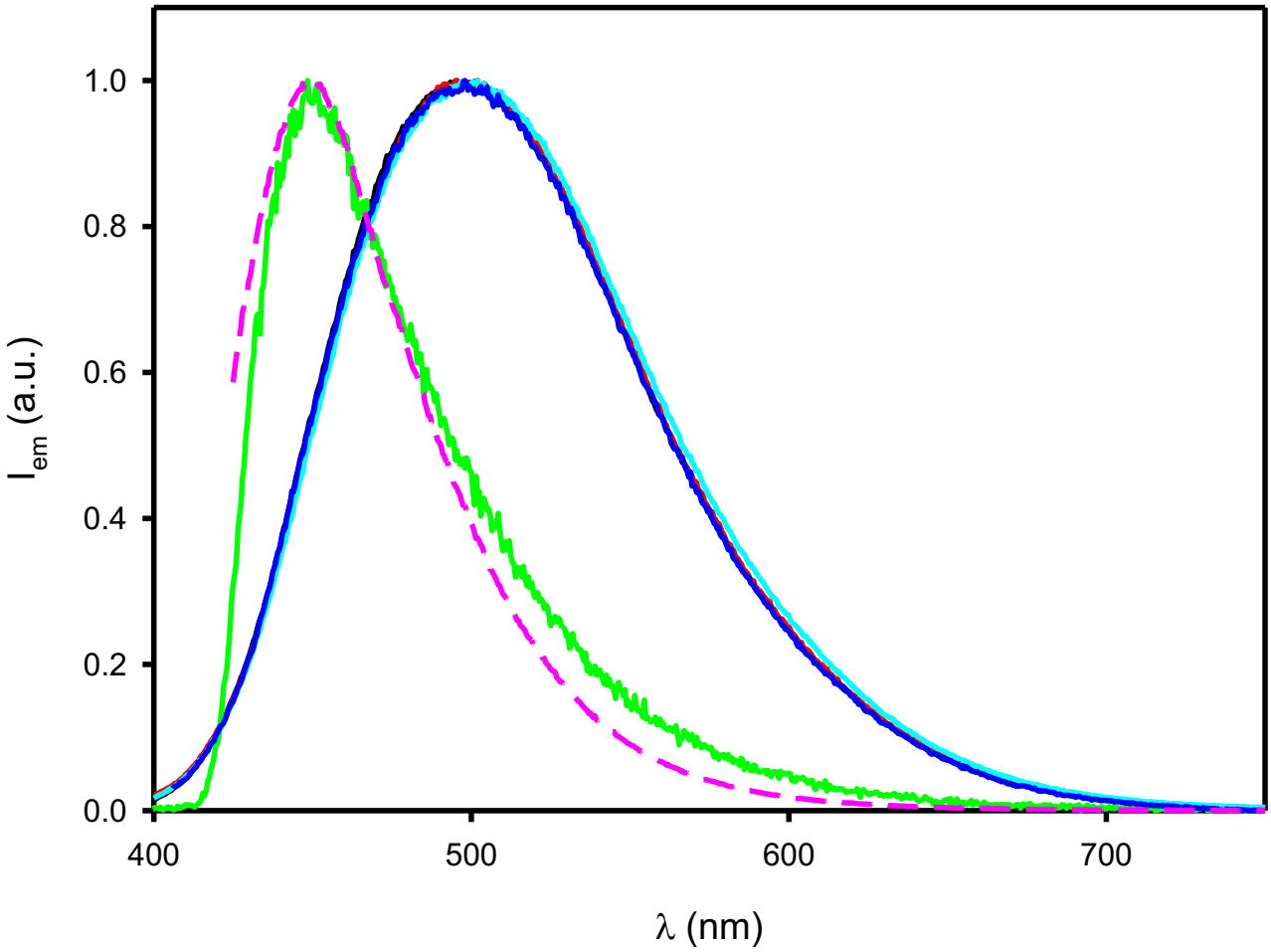

Figure **S8**. Normalized emission spectra of a 4.27×10^{-5} M solution of **pDTCz-DPmS** in THF (black) and after the addition of PhCCBr (red, 3.7 mM), HE (green, 3.9 mM), NHPI (cyan, 4.1 mM), DIPEA (blue, 3.5 m) and emission spectrum of a 2.55×10^{-3} M solution of HE in THF (pink dashed), where λ_{exc} = 390 nm in all cases.

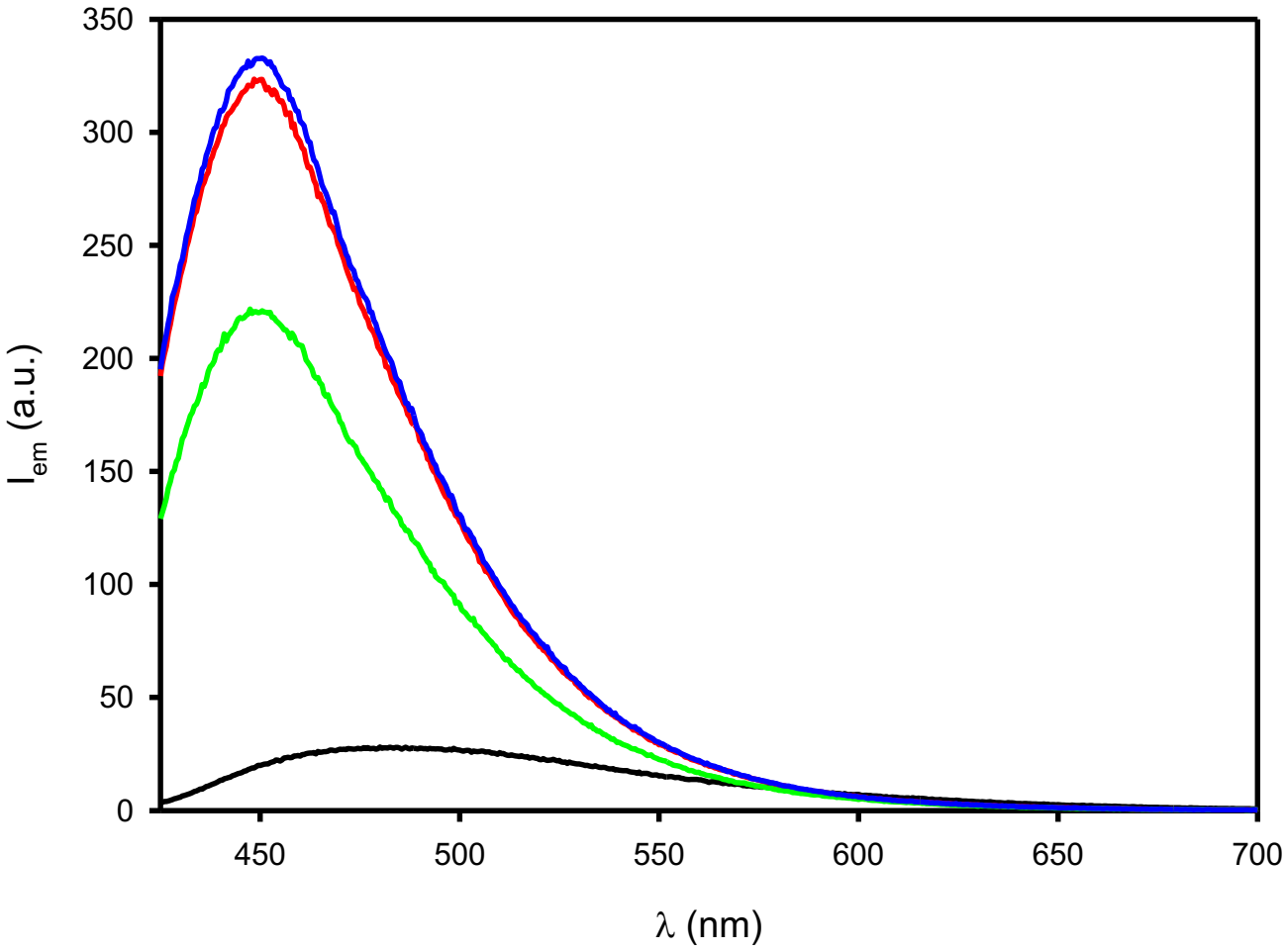

Figure **S9**. Emission spectra of a 2.55×10^{-3} M solution of HE in THF (blue) and after the addition of PhCCBr (black, 200 mM), NHPI (green, 300 mM), DIPEA (red, 400 mM), where λ_{exc} = 390 nm in all cases.

Quenching studies

To evaluate the quenching of **pDTCz-DPmS** under the reaction conditions, we evaluated the quenching efficiency of species *i* according to the following formula:

$$\eta^i = \frac{k_q^i \cdot [Q]^i}{k_{nr} + k_r + \sum_0^n k_q^i \cdot [Q]^i} \cdot 100$$

where $k_{nr} + k_r = \frac{1}{\tau^0}$ are the intramolecular deactivation pathways and k_q^i is the quenching constant of the quencher species *i*.

We can evaluate the weight of the prompt and delayed emission quenching by the ratio of the quenching efficiency corrected by the ratio of the populations of the triplet and singlet states of the photocatalyst according to the following formulas:

$$\chi^S = \frac{\Phi_{PROMPT}}{\Phi_{TADF}} \qquad \chi^T = 1 - \frac{\Phi_{PROMPT}}{\Phi_{TADF}}$$

Where χ^S and χ^T are the populations of singlet and triplet excitons for **pDTCz-DPmS**.

$$\mathrm{X}^{PROMPT} = \frac{\tau_0^{PROMPT} \cdot k_{qPROMPT}^i \cdot \chi^S}{\tau_0^{PROMPT} \cdot k_{qPROMPT}^i \cdot \chi^S + \tau_0^{TADF} \cdot k_{qTADF}^i \cdot \chi^T} \cdot 100$$

$$\mathrm{X}^{TADF} = \frac{\tau_0^{TADF} \cdot k_{qTADF}^i \cdot \chi^T}{\tau_0^{PROMPT} \cdot k_{qPROMPT}^i \cdot \chi^S + \tau_0^{TADF} \cdot k_{qTADF}^i \cdot \chi^T} \cdot 100$$

Where X^{PROMPT} and X^{TADF} are the weight of prompt and TADF emission in quenching process, τ_0^{PROMPT} and τ_0^{TADF} are the lifetime of the pristine and delayed fluorescence of **pDTCz-DPmS**, $k_{qPROMPT}^i$ and k_{qTADF}^i are the quenching constant for a specific quencher i for prompt and TADF emission.

NMR studies

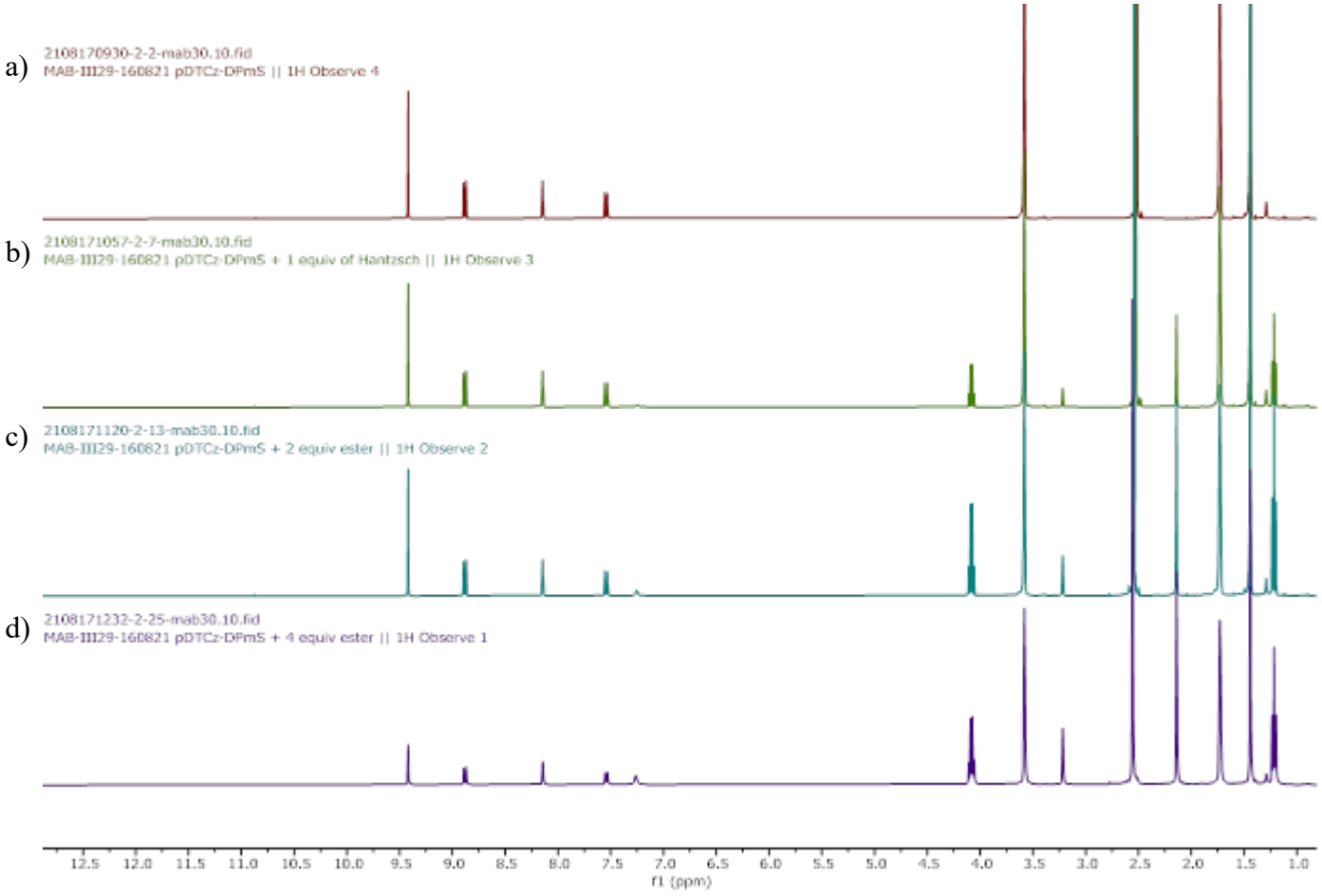

Figure **S10**. ^{1}H NMR spectra of **pDTCz-DPmS** with a) 0, b) 1, c) 2 and d) 4 equivalents of HE, all in THF-d_8.

The insensitivity of the ^{1}H NMR spectrum of **pDTCz-DPmS** with increasing amounts of HE implies that there is no new species formed between the two compounds in the ground state. Only 4 equivalents of HE could be added before the concentration became too high for the resonances to be resolved clearly.

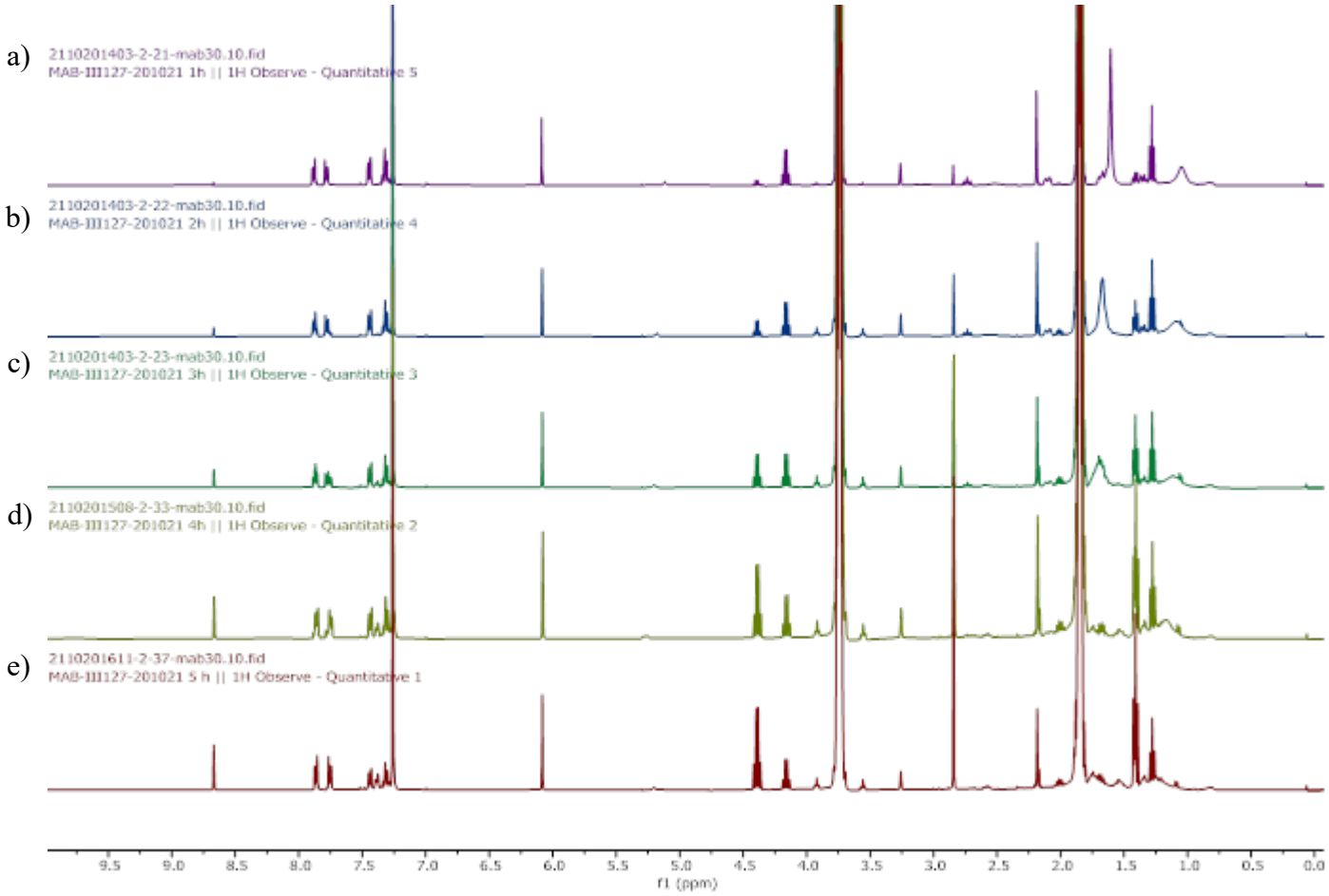

Figure **S11**. ^{1}H NMR spectra of C(sp)-C(sp^{3}) cross coupling reaction in the absence of photocatalyst monitored at a) 1 h, b) 2 h, c) 3 h, d) 4 h and e) 5 h. The reaction was completed in THF and the ^{1}H NMR spectra obtained in $CDCl_3$.

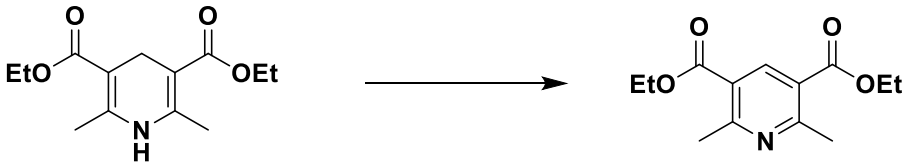

Figure **S12**. Chemical structures of the Hantzsch ester (left) and the oxidised Hantzsch ester (right).

References

1 M. A. Bryden, F. Millward, T. Matulaitis, D. Chen, M. Villa, A. Fermi, S. Cetin, P. Ceroni and E. Zysman-Colman, *J. Org. Chem.*, 2023, **88**, 6364–6373.

2 L. M. Schneider, V. M. Schmiedel, T. Pecchioli, D. Lentz, C. Merten and M. Christmann, *Org. Lett.*, 2017, **19**, 2310–2313.

3 A. Peterson, M. Kaasik, A. Metsala, I. Järving, J. Adamson and T. Kanger, *RSC Adv.*, 2019, **9**, 11718–11721.

4 J. Cornella, J. T. Edwards, T. Qin, S. Kawamura, J. Wang, C. M. Pan, R. Gianatassio, M. Schmidt, M. D. Eastgate and P. S. Baran, *J. Am. Chem. Soc.*, 2016, **138**, 2174–2177.

5 J. N. Demas and G. A. Crosby, *J. Phys.*, 1971, **75**, 991–1024.

6 K. Suzuki, A. Kobayashi, S. Kaneko, K. Takehira, T. Yoshihara, H. Ishida, Y. Shiina, S. Oishi and S. Tobita, *Phys. Chem. Chem. Phys.*, 2009, **11**, 9850–9860.